Journal of Molecular Catalysis A: Chemical 309 (2009) 40–49

Contents lists available at ScienceDirect

Journal of Molecular Catalysis A: Chemical

journal homepage: www.elsevier.com/locate/molcata

Particle growth and fragmentation of solid self-supported Ziegler–Natta-type catalysts in propylene polymerization

Hanna-Leena Rönkkö[a], Tarmo Korpela[a], Hilkka Knuuttila[a], Tuula T. Pakkanen[a,*], Peter Denifl[b], Timo Leinonen[b], Marianna Kemell[c], Markku Leskelä[c]

[a] Department of Chemistry, University of Joensuu, P.O. Box 111, FI-80101 Joensuu, Finland
[b] Borealis Polymers Oy, P.O. Box 330, FI-06101 Porvoo, Finland
[c] Department of Chemistry, Laboratory of Inorganic Chemistry, University of Helsinki, P.O. Box 55, FI-00014 Helsinki, Finland

ARTICLE INFO

Article history:
Received 9 January 2009
Received in revised form 20 April 2009
Accepted 22 April 2009
Available online 3 May 2009

Keywords:
Ziegler–Natta catalyst
Propylene polymerization
Catalyst fragmentation
$MgCl_2$

ABSTRACT

Particle growth and fragmentation of solid Ziegler–Natta-type catalysts prepared via emulsion technique were studied in propylene polymerization. Before polymerizations the catalyst particles were activated with triethyl aluminum (TEA) and cyclohexyl methyl dimethoxy silane (CMMS). Polymerizations were carried out in gas-phase in a micro-reactor system that allows the particle growth to be observed with a microscope. Several polymerizations were done under a propylene pressure of 2 bar and with polymerization times from 20 s to 2 h. Fragmentation morphology of the catalyst particles and cross-sections of the particles after polymerization were studied by scanning electron microscopy/energy dispersive spectroscopy (SEM/EDS). Fragmentation morphology of the catalysts prepared via emulsion technique was compared with the fragmentation morphology of a conventional $MgCl_2$-supported Ziegler–Natta-type catalyst, which could be described by the multigrain model. Polymer growth appeared to occur throughout the emulsion-based catalyst particle right from the start of the polymerization, even though the surface area and porosity of the catalyst were low. The surface of the catalyst particles broke up at the beginning of the polymerization, and catalyst fragments appeared on the surface as plates between which the polymer was growing.

1. Introduction

Polyethylene (PE) and polypropylene (PP) are typically produced with Ziegler–Natta catalyst systems [1–3], but how the Ziegler–Natta system really works is not entirely clear. Better understanding of the behavior would offer significant support to catalyst design and development. Catalyst polymerization and fragmentation behavior greatly depend on the type of catalyst and the nature of the catalyst support [4]. It is widely believed that the catalyst needs to be highly porous so that the monomer can diffuse into the particle. The mechanical strength of the catalyst structure must be high enough to withstand handling of the catalyst, but at the same time low enough to break up in polymerization. Fragmentation of catalyst particles affords higher polymer yields and ensures absence of big catalyst fragments in the final product. The active sites should also be well distributed over the catalyst particle so that the polymer is evenly formed within the catalyst [4–6].

The growth and the fragmentation of catalyst particles in olefin polymerization have been studied by several research groups [4,7–19], and at least three different models for particle morphology in polymer growth have been presented. In the core–shell model, also known as the layer-by-layer model, the catalyst particle does not break up at the beginning of the polymerization process. The polymerization reaction occurs on the surface of the particle, which acts as a core, and the polymer grows in the form of a shell around the core. The monomer diffuses through the accumulated polymer to the catalyst surface, where it reacts [4,20–24]. According to some investigations [8,9], this kind of polymer growth proceeds in slurry-phase propylene polymerization if the porosity of the catalyst is low (monomer diffusion is limited). In the case of a highly porous catalyst the monomer diffusion is less limited; the monomer can penetrate into the pores of the catalyst more easily and the polymer grows throughout the particle. The result is an immediate fragmentation of the catalyst particle [8,9]. This particle morphology model, known as the multigrain model, is one of the most popular and simple models for the particle growth in olefin polymerization [25]. According to the multigrain model, immediately when the

* Corresponding author. Tel.: +358 13 251 3340; fax: +358 13 251 3390.
E-mail addresses: hanna-leena.ronkko@joensuu.fi (H.-L. Rönkkö), tarmo.korpela@joensuu.fi (T. Korpela), hilkka@knuuttila.fi (H. Knuuttila), tuula.pakkanen@joensuu.fi (T.T. Pakkanen), peter.denifl@borealisgroup.com (P. Denifl), timo.leinonen@borealisgroup.com (T. Leinonen), marianna.kemell@helsinki.fi (M. Kemell), markku.leskela@helsinki.fi (M. Leskelä).

1381-1169/$ – see front matter © 2009 Elsevier B.V. All rights reserved.
doi:10.1016/j.molcata.2009.04.013

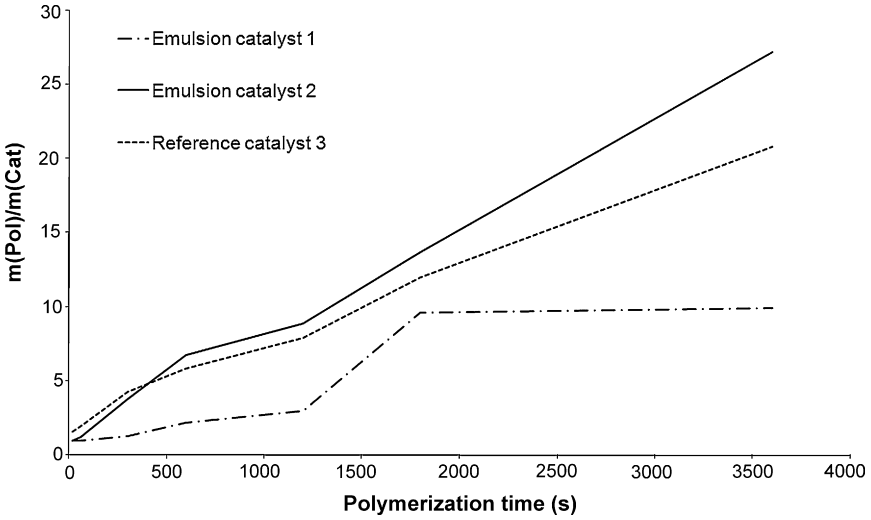

Fig. 1. Polymer/catalyst mass ratios of the polymerizations as a function of the polymerization time.

polymerization starts the catalyst particles break up into small fragments (microparticles), and the polymerization reaction occurs on the surface of these microparticles following the core–shell model. The microparticles together form porous macroparticles [22,24,25]. The third model is the polymeric flow model. According to this model it is also assumed that the catalyst particles break up at the beginning of the polymerization [24]. Polymer and catalyst fragments are considered as one phase, and the polymerization reaction occurs at active sites which are embedded in the polymer and are moving radially outward with the forming polymer [23,24]. The multigrain and polymeric flow models are the models most commonly used to explain the replication phenomena [7].

Various models for particle fragmentation have been presented in the literature [15,16,24,26]. One fragmentation model is a continuous bisection fragmentation model, where the catalyst carrier successively fragments into finer and finer fragments [16,26]. In the case of shrinking core model, fragmentation proceeds from the surface to the center of the particle [15,26]. According to the studies of Hammawa and Wanke [27] the fragmentation mechanism of less fragile catalysts is the shrinking core, whereas highly friable catalysts follow the continuous bisection fragmentation model [26,27].

Abboud et al. [12–14] have studied the fragmentation behavior and replication of the emulsion-based Ziegler–Natta catalyst in gas- and slurry-phase propylene polymerizations. The behavior of the emulsion-based catalyst was compared with that of $MgCl_2$-supported [12] and silica-supported [13,14] catalysts of similar chemical composition. Polymerizations were carried out for different polymerization times and under different polymerization conditions (time and temperature), and fragmentation of the catalyst samples was studied by melting the polymer particles and observing them under a microscope. According to these studies, the fragmentation of the emulsion-based catalyst was faster and more uniform than that of the $MgCl_2$- and silica-supported catalysts.

The aim of our study was to determine the fragmentation mechanism of the emulsion-based Ziegler–Natta catalyst. Main focus was on the initial steps of the polymerization and the fragmentation pattern of three Ziegler–Natta catalysts. Two solid self-supported Ziegler–Natta-type catalysts (emulsion-based catalysts **1** and **2**) prepared by emulsion technique [28,29] and a $MgCl_2$-supported conventional reference catalyst (catalyst **3**) [30] for propylene polymerization were studied. Catalysts were of similar chemical composition, but differed in method of preparation. The two emulsion-based catalyst samples differed from each other only in

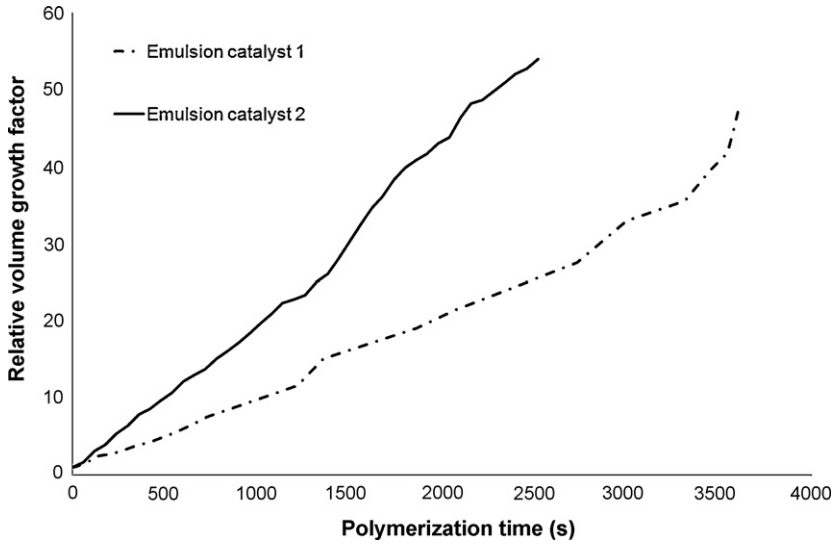

Fig. 2. Relative volume growth factor as a function of polymerization time (calculated as the average volume of the polymer particles to the average volume of the catalyst particles).

that a small amount of aluminum alkyl compound was used in the washing step of catalyst **2** [29]. The surface area of the two emulsion-based catalysts is exceptionally low (about 2 m^2/g) [31], but the polymerization activity is high. This high activity can be explained by the chain-like inner structure, with the chains extending from the center of the particle to the surface [31]. Because of this inner structure, the monomer probably does not encounter diffusion problems during the polymerization. All polymerizations of the study were carried out in gas-phase in a micro-reactor system that allows the polymer particle growth to be followed with a video microscope. Fragmentation morphology and the cross-sections of the polymer particles were studied by SEM and SEM/EDS.

2. Experimental

2.1. Preparation of catalyst samples

The emulsion-based catalyst samples **1** and **2**, and also the reference catalyst sample (catalyst **3**), were supplied by Borealis Polymers Oy. Catalyst synthesis via emulsion method consists of three stages. In the first stage a liquid/liquid two-phase system is formed where one phase is a solution of the catalyst components in an inert solvent. In the first step of stage 1, butyl octyl magnesium (BOMAG) and 2-ethyl-1-hexanol were reacted to magnesium alkoxide. Next the magnesium alkoxide was allowed to react with phthaloyl dichloride (PDC), and $MgCl_2$/di(ethylhexyl)phthalate (DEHP) was formed. In the final step of stage 1, the $MgCl_2$/DEHP complex was reacted with $TiCl_4$ and a liquid/liquid two-phase system was formed. In the second stage the catalyst droplets were stabilized through addition of a surfactant and emulsification occurred. The third stage, the solidification of the catalyst droplets, was achieved by changing the reaction conditions of the emulsion system. The catalyst particles were isolated and dried [28]. Synthesis of the emulsion-based catalyst **2** was the same as that of catalyst **1**, but a small amount of aluminum alkyl was added in the washing step [29]. The reference catalyst (catalyst **3**) was synthesized by conventional method: the $MgCl_2$ was reacted with alcohol and then the adduct of $MgCl_2$ and alcohol was melted and crystallized (spray crystallization). The crystallized adduct is used as a carrier onto which the $TiCl_4$ and dialkylphthalate are impregnated [30].

2.2. Polymerizations

The propylene gas-phase polymerizations were carried out in a house-made 10-ml micro-reactor. Before polymerizations the catalyst samples were activated with cocatalyst triethyl aluminum (TEA) and external electron donor cyclohexyl methyl dimethoxy silane (CMMS). Al/Ti and Al/CMMS mole ratios were 250 and 10 mol/mol, respectively. First, the TEA (mixed with n-pentane) was allowed to react with CMMS for about 5 min and then the mixture was added to the catalyst. After reaction of about 10 min, the catalyst sample was washed with n-pentane and dried. Polymerizations with different times were carried out using the same activated batch of the catalyst. After the activation reaction, a small amount of the catalyst was weighed into the reactor and the reactor was enclosed in a glove box. After weighing, the reactor was brought out of the glove box and connected to the propene line. The propene gas was purified with three commercial purifiers and one self-made silica/MAO purifier. The polymerization times ranged from 20 s to 2 h. Polymerization temperature was 50 °C and the monomer (propene, 99.995%) pressure was 2 bar. Activities of the polymerizations were observed by weighing the catalyst/polymer particles before and after the polymerization. Also, relative volume growth factors of the particles were determined from the diameters of the catalyst and polymer particles viewed with a video microscope.

2.3. Scanning electron microscopy

Catalyst/polymer particles and the cross-sections of the catalyst/polymer particles were studied with high-resolution Hitachi

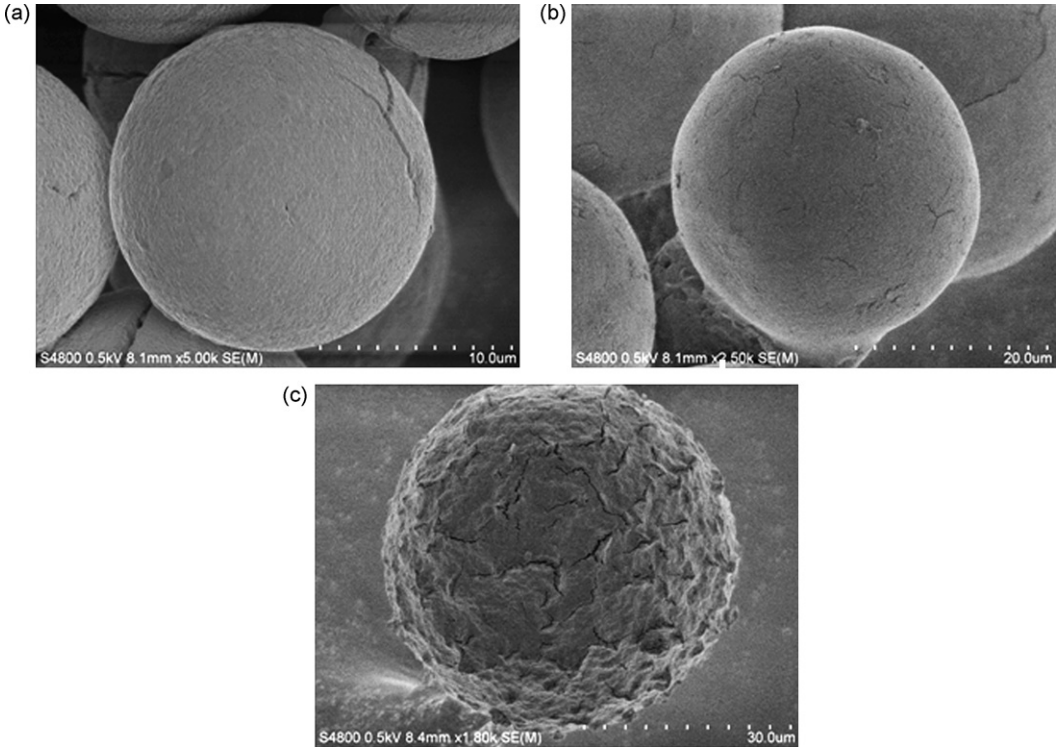

Fig. 3. SEM images of catalyst particles: (a) emulsion-based catalyst **1**, (b) emulsion-based catalyst **2**, and (c) reference catalyst **3**.

S-4800 field emission scanning electron microscopes (at the University of Joensuu and the University of Helsinki). For preparation of the cross-sections, the samples were mixed with resin (SPI Supplies epoxy resin) under a nitrogen atmosphere. The resin/sample mixtures were cured from a few days to a few weeks. The cross-sections were cut with a microtome (LeicaRM2165). Thickness of the cross-cuts was in the range of 10–40 μm. Before SEM measurements the samples were coated with carbon, Pt/Pd mixture, or gold (2 nm coating). The coatings were used to prevent charging of the samples. In the case of short polymerization times, catalyst/polymer samples were sealed in an inert vial in the glove box, and just before SEM measurements they were fixed on a tape and quickly moved to the chamber of the SEM to prevent their contact with air and moisture. Energy dispersive X-ray (EDX) analysis mappings, with a Thermo Electron Corporation Noran System Six, were carried out at the University of Joensuu.

3. Results and discussion

3.1. Polymerization activities of the catalysts

Activities of the catalysts were assessed as mass of polymer to mass of catalyst used in the gas-phase polymerization of propene. Fig. 1 shows the results as a function of polymerization time from 20 s to 1 h. Polymer yields of the emulsion-based catalyst **2** and reference catalyst **3** appear to be higher than those of emulsion-based catalyst **1**. Polymer yields obtained differ from those of the industrial processes because of the different polymerization conditions. In our study a gas-phase was used instead of slurry-phase and also temperature and propene pressure were lower than those in the industrial case. Fig. 2 shows the relative volume growth factors (average volume of the polymer particles to average volume of the catalyst particles) for the emulsion catalysts **1** and **2** as a function

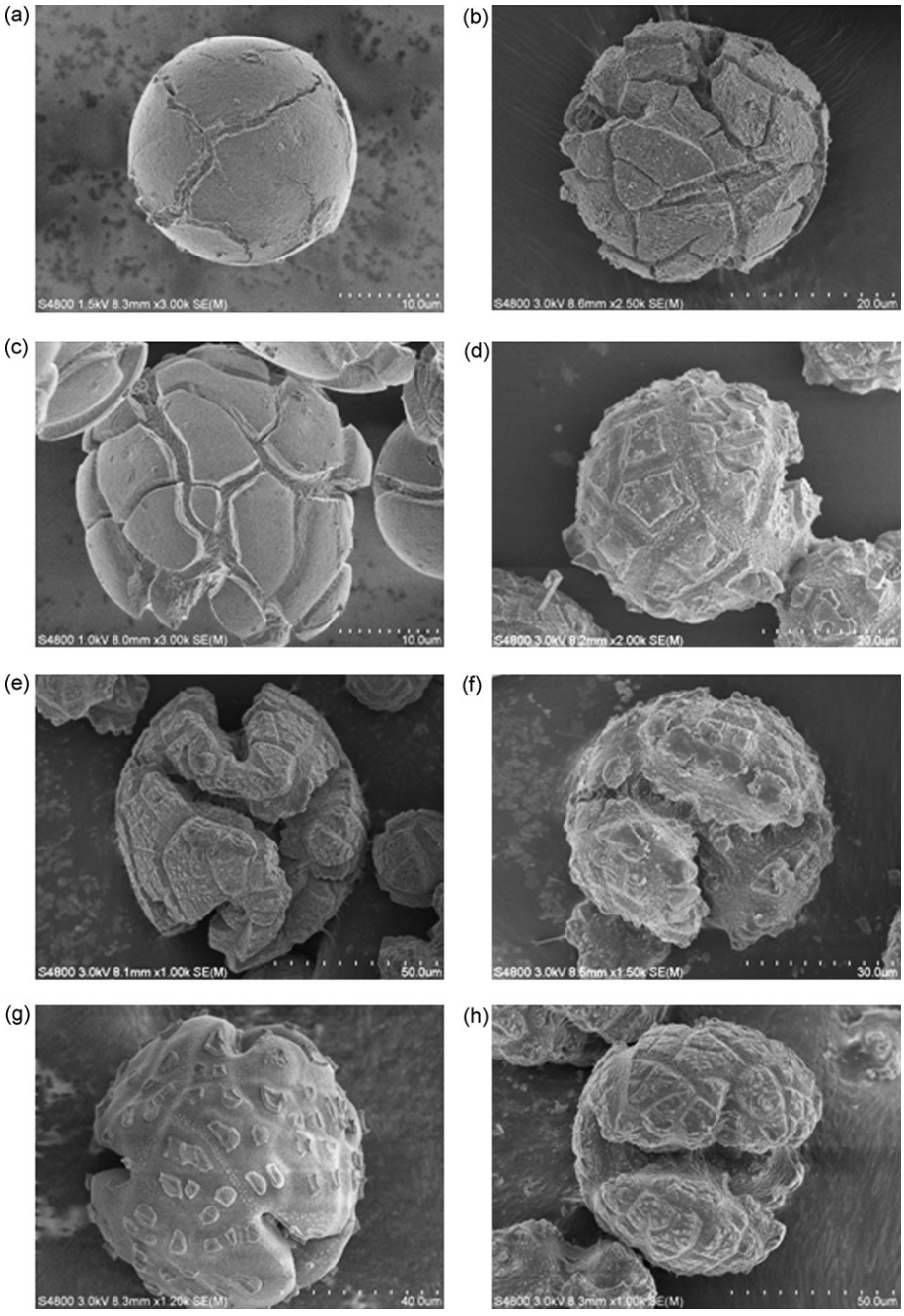

Fig. 4. SEM images of polymer particles polymerized with emulsion-based catalyst **1** for (a) 20 s, (b) 1 min, (c) 5 min, (d) 10 min, (e) 20 min, (f) 30 min, (g) 1 h, and (h) 2 h.

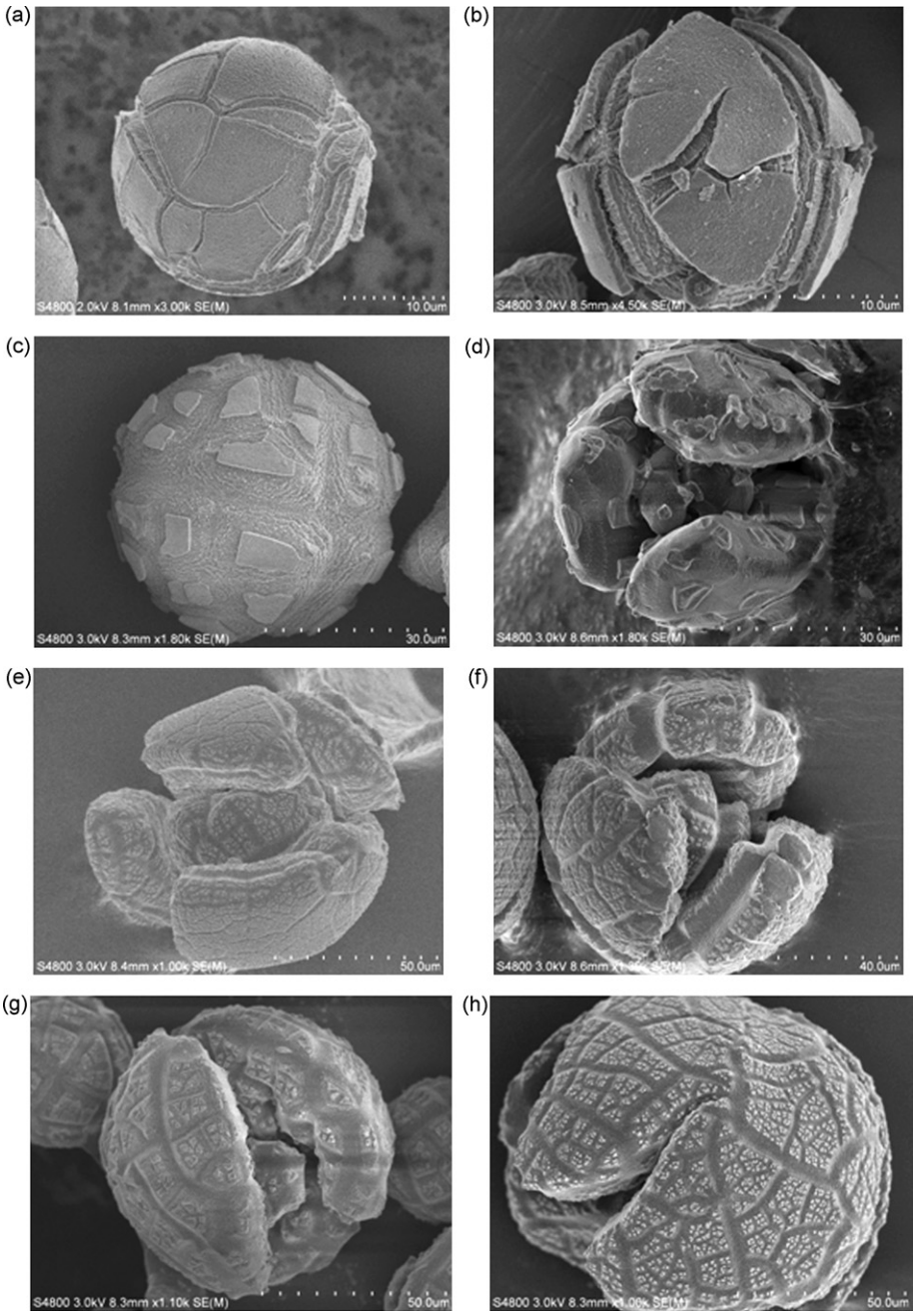

Fig. 5. SEM images of polymer particles polymerized with emulsion-based catalyst **2** for (a) 20 s, (b) 1 min, (c) 5 min, (d) 10 min, (e) 20 min, (f) 30 min, (g) 1 h, and (h) 2 h.

of polymerization time (20 s to 1 h). Diameters of the catalyst and polymer particles were estimated from microscopy images. Relative volume growth factors of the emulsion catalysts **1** and **2** follow roughly the same trend as the activity curves of the catalysts (Fig. 1). Relative volume growth factors of the emulsion catalyst **2** are higher than those of the emulsion catalyst **1**.

3.2. Fragmentation morphology of the catalyst and polymer particles

Fragmentation morphology of the catalyst and polymer particles was studied by monitoring the growth of the polymer particles by SEM and SEM/EDS. Fig. 3 shows SEM images of the initial catalyst particles. The surfaces of the emulsion-based catalyst particles appear smooth, while the surface of the reference catalyst is rough with visible cracks. The particle size of the reference catalyst (50–100 μm) is also larger than that of the emulsion-based catalysts (20–50 μm). SEM images of the polymer particles after 20 s to 2 h polymerizations with the three catalysts are presented in Figs. 4–6. Polymer particles produced with the emulsion-based catalysts **1** and **2** appear to break increasingly during the polymerization process (Figs. 4e and f and 5d–f). In contrast, the reference catalyst (catalyst **3**) maintains its spherical morphology during the gas-phase polymerization (Fig. 6).

After just 20 s polymerization, cracks could be seen on the surface of the particles of the emulsion-based catalysts (Figs. 4a and 5a). The fragmentation increases with the polymerization time as the surface of the particles continues to fracture. The surfaces are fragmented into plates, and the plates break into smaller and smaller pieces as the polymerization proceeds. According to EDS measurements, the plates mainly consist of catalyst material; this is clearly seen in Fig. 7, which presents SEM/EDS

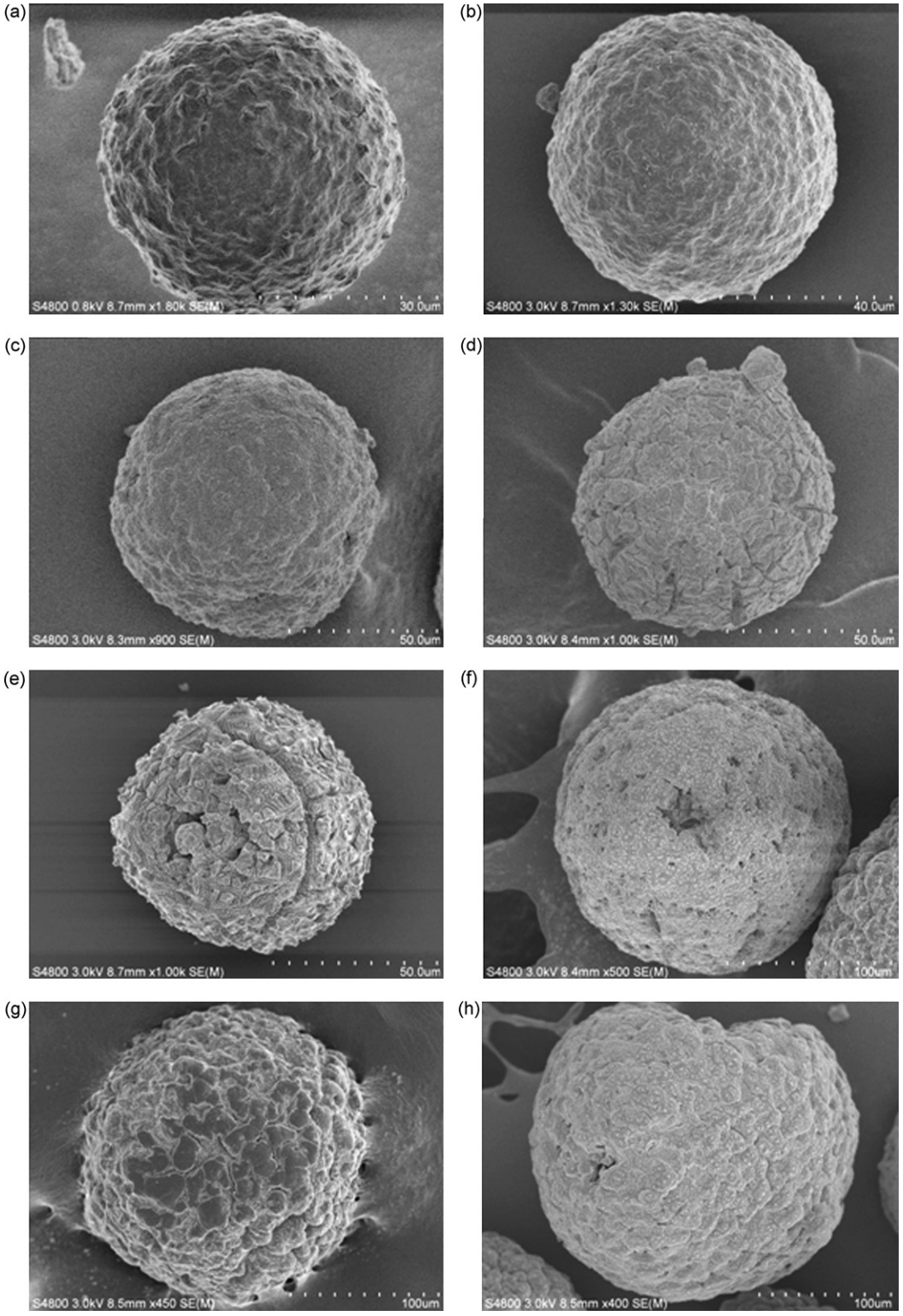

Fig. 6. SEM images of polymer particles polymerized with the reference catalyst (catalyst **3**) for (a) 20 s, (b) 1 min, (c) 5 min, (d) 10 min, (e) 20 min, (f) 30 min, (g) 1 h, and (h) 2 h.

elemental maps of the surface of a polymer particle polymerized with emulsion-based catalyst **2** for 10 min. The plates mainly consist of magnesium and chlorine, while the gaps between the plates mainly consist of carbon. Fig. 8 presents SEM/EDS mappings of the surface of a polymer particle after longer polymerization (emulsion-based catalyst **2** after 30 min polymerization). The plates on the surface are now broken into smaller pieces. Although the plates still mainly consist of magnesium and chlorine, the carbon appears to be evenly distributed over the whole area. Andoni et al. [32–34] have noticed in their studies that the polymer grows at the edges and corners of the catalyst crystallites. Also here the polymerization appears to take place at the edges of the plates, and as a consequence of the polymerization the plates are broken into smaller fragments. Similar results were obtained in the SEM/EDS

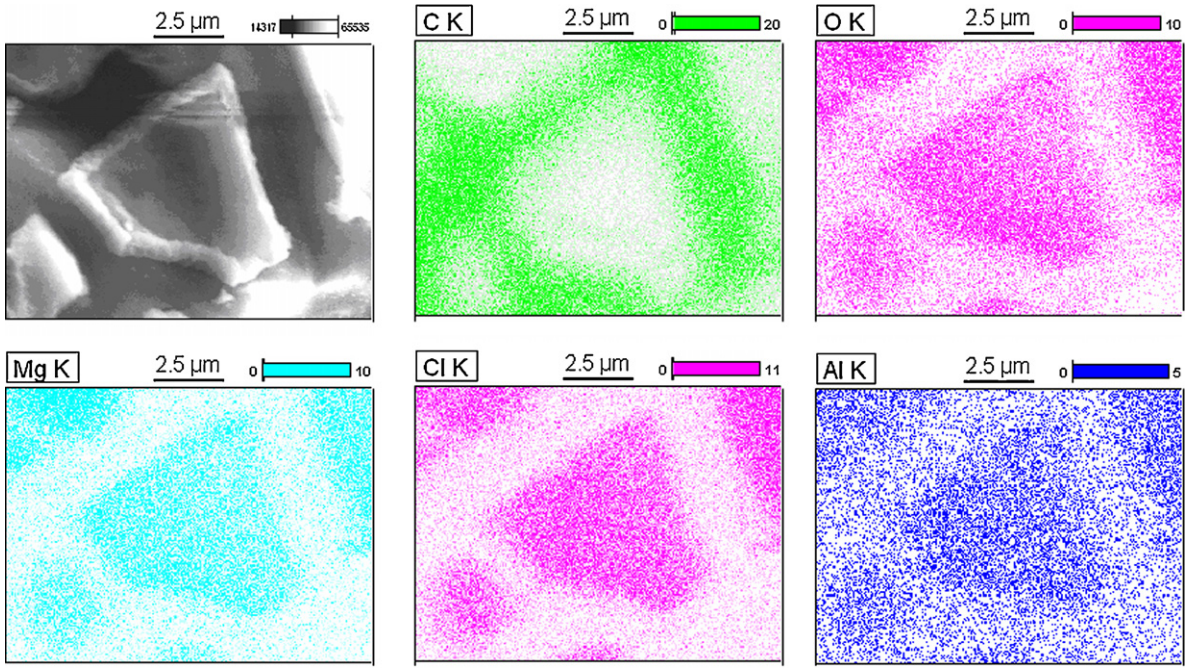

Fig. 7. SEM/EDS elemental mappings of the surface of a polymer particle polymerized with emulsion-based catalyst **2** for 10 min.

mappings of the polymer particles polymerized with emulsion catalyst **1**. Fig. 9 shows SEM images of the surfaces of polymer particles after 10 min polymerization with the three catalysts. Polymer fibers between the plates can be seen on the surface of the polymer particles produced by emulsion-based catalysts **1** and **2** (Fig. 9a and b). According to the morphology of the polymer particle produced by emulsion-based catalysts (catalyst **1** and **2**), at the initial stage of the polymerization the outer layer of the catalyst particle is first fragmented. Then the next layer starts cracking and the fragmentation proceeds through the catalyst particle. Fragments of the outer layer keep fragmenting into smaller pieces. The fragmentation of the emulsion-based catalyst particles is best described by the continuous bisection fragmentation model presented by Kosek and co-workers [26], where the catalyst carrier successively fragments into finer and finer fragments.

The fragmentation pattern of the reference sample (catalyst **3**) differs from that of the emulsion-based catalysts. Particles retain their spherical morphology and evidently expand in a controlled way, which supports the fragmentation resulting in multigrain morphology. According to the multigrain model it is assumed that the

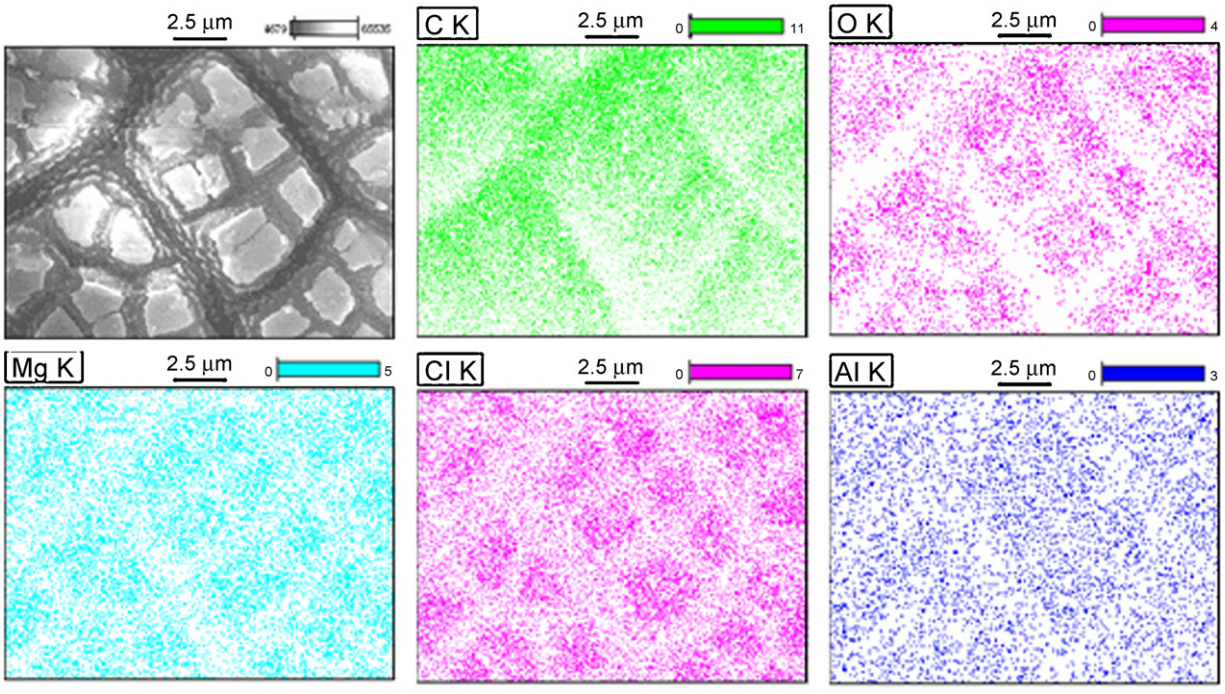

Fig. 8. SEM/EDS elemental mappings of the surface of a polymer particle polymerized with emulsion-based catalyst **2** for 30 min.

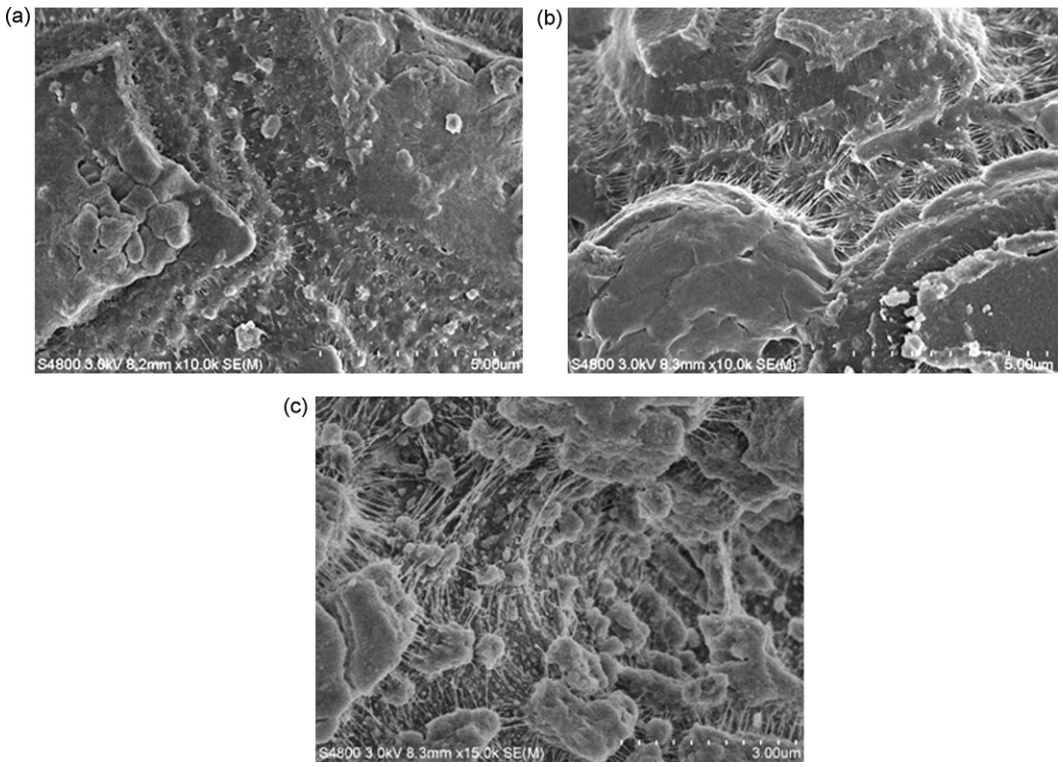

Fig. 9. SEM images of the surface of the polymer particles after 10 min polymerization: (a) emulsion-based catalyst **1**, (b) emulsion-based catalyst **2**, and (c) reference catalyst (catalyst **3**).

catalyst particle breaks into smaller microparticles right from the beginning of the polymerization. Each microparticle acts as a polymerizing agent and the microparticles are held together by the growing polymer mass. At 10 min, the surface of the polymer particle polymerized with the reference catalyst **3** (Fig. 9c) exhibits polymer fibers between the microparticles. Fig. 10 presents EDS spectra recorded from the surface of the polymer particles grown with the reference catalyst (catalyst **3**) in 1 h. As can be seen, point 1, measured in a gray area, mainly consists of carbon and indicates polymer. EDS spectra of points 2, 3, and 4, measured from

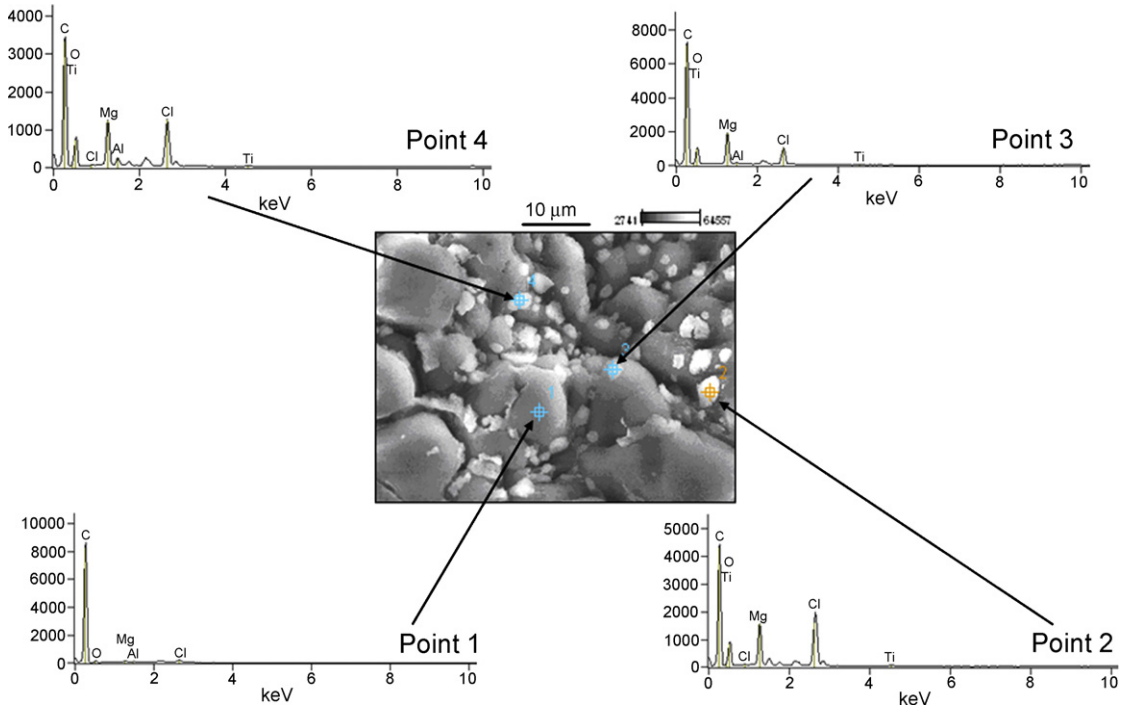

Fig. 10. EDS spectra measured by point and shoot method from the surface of the polymer particle obtained with the reference catalyst (catalyst **3**) after 1 h polymerization.

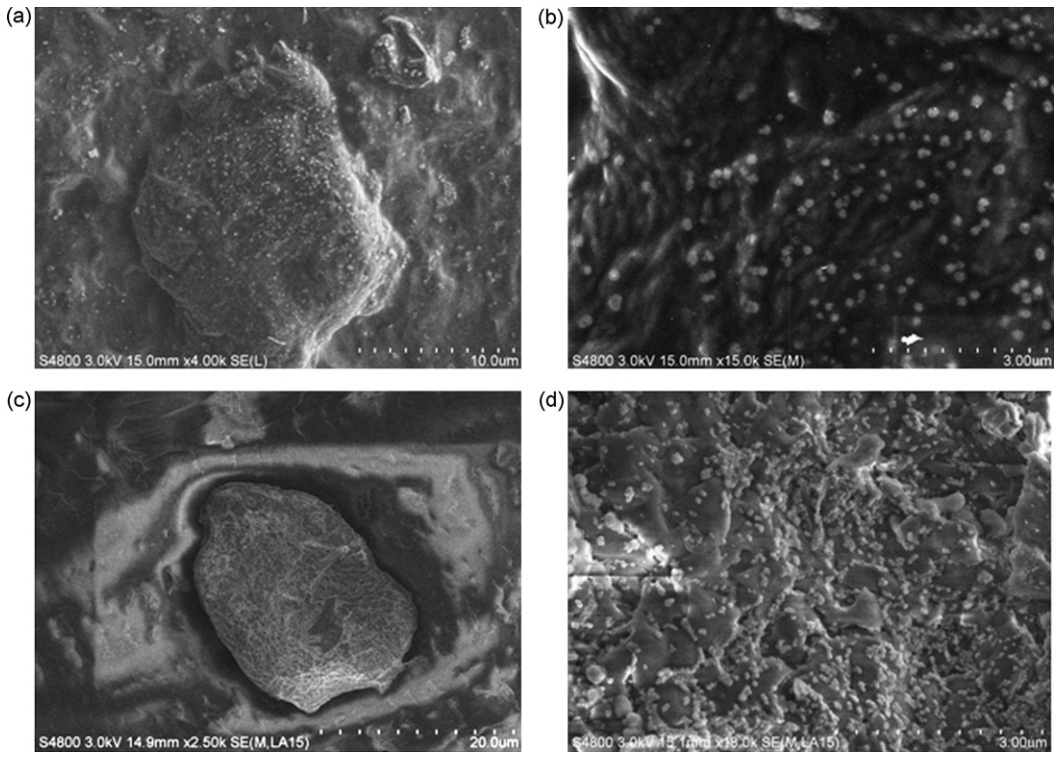

Fig. 11. Cross-sections of emulsion-based catalyst/polymer particles (in epoxy resin) after 1 min polymerizations. (a) Emulsion-based catalyst **1**, (b) magnification of image (a), (c) emulsion-based catalyst **2**, and (d) magnification of image (c).

light-colored flakes with diameters of 1–5 μm, reveal the signals of magnesium and chlorine and indicate catalyst material.

3.3. Cross-sections of the polymer particles

Fig. 11 presents SEM images of cross-sections of the polymer particles (in epoxy resin) after 1 min polymerizations with the emulsion-based catalysts **1** and **2**. The spherical dots of size 50–100 nm on the surface of the cross-cuts probably are polypropylene particles. Since the amount of these species is higher on the cross-section of catalyst **2**, it can be concluded that after 1 min polymerization the activity or the fragmentation rate of catalyst **2** is higher than that of catalyst **1** under the test conditions. This is in good agreement with the activity values of these two catalysts (Figs. 2 and 3). The amount of spherical polymer particles also increases with the polymerization time. Since the small spherical particles are distributed through the whole catalyst particles, we conclude that also the polymerization takes place through the whole catalyst particle.

Abbound et al. [12] concluded that the fragmentation of the emulsion-based catalyst in propylene gas-phase polymerization is faster and more uniform than that of $MgCl_2$-supported catalyst. Our studies indicate similarly that the fragmentation of the emulsion-based catalyst particles is faster than the fragmentation of the $MgCl_2$-supported reference catalyst. We also observed that the fragmentation of the emulsion-based catalyst particles begins immediately when the polymerization starts, and that the polymerization appears to take place throughout the catalyst particles despite their low porosity. These findings, together with the new information about the catalyst material on the surface of the polymer particles provided by SEM/EDS mappings, lead us to propose that catalyst fragments are distributed throughout the polymer particle, and catalyst fragments, originating from the plates that are broken into smaller fragments as the polymerization proceeds, occur on the surface of the polymer particles. This, again, can be described by the continuous bisection fragmentation model.

4. Conclusions

The fragmentation behavior of emulsion-based catalyst particles and reference catalyst particles were studied in propylene gas-phase polymerization. The polymer yields of the emulsion-based catalyst **2** and reference catalyst **3** were higher than the polymer yield of the emulsion-based catalyst **1**. Relative volume growth factors of the emulsion-based catalyst particles (catalysts **1** and **2**) follow the same trend as the activity curve, showing higher growth values for emulsion-based catalyst **2** than emulsion-based catalyst **1**. The surface of the emulsion-based catalysts begins to crack at the outset of the polymerization, after just 20 s. Plates appear on the surface after a short while, and as the polymerization proceeds they break up into increasingly smaller pieces. According to SEM/EDS studies, the plates on the surface consist of catalyst material (Mg and Cl), while the polymer grows in the gaps between the plates and apparently on the lateral faces on the plates. The fragmentation of the emulsion-based catalyst particles is best described by the continuous bisection fragmentation model. The fragmentation of the reference catalyst (catalyst **3**) behaves differently, and judging from the morphology of the polymer particles, is better described by the multigrain morphology. Particles retain their spherical morphology and expand evenly throughout the polymerization. SEM/EDS images revealed flakes of catalyst material 1–5 μm in diameter over the whole surface of the reference catalyst particle. SEM study of cross-sections of the nascent polymer particles polymerized for 1 min with the emulsion-based catalysts revealed spherical particles 50–100 nm in diameter evenly distributed over the cross-sectional surface, indicating that the polymerization commenced simultaneously through the whole catalyst particle. Hence, despite of the low surface area and porosity, polymerization in the

emulsion-based catalyst particle occurs throughout the particle, not only on the surface. This finding also supports the conclusion that the fragmentation of the emulsion-based catalyst particles is best described by the continuous bisection model.

Acknowledgements

We are grateful to Borealis Polymers Oy for funding the research and supplying the catalyst samples. Dr. Jani Turunen and Mr. Kalle Kallio are thanked for their assistance in development of the polymerization micro-reactor system.

References

[1] N. Kashiwa, J. Polym. Sci. A: Polym. Chem. 42 (1–8) (2004) 1.
[2] J.J.A. Dusseault, C.C. Hsu, J. Macromol. Sci. Rev. Macromol. Chem. Phys. C 33 (2) (1993) 103.
[3] S. Kojoh, T. Fujita, N. Kashiwa, Recent Res. Dev. Polym. Sci. 5 (2001) 43.
[4] J.T.M. Pater, G. Weickert, J. Loos, W.P.M. van Swaaij, Chem. Eng. Sci. 56 (2001) 4107.
[5] J.T.M. Pater, G. Weickert, W.P.M. van Swaaij, J. Appl. Polym. Sci. 87 (2003) 1421.
[6] G. Weickert, G.B. Meier, J.T.M. Pater, K.R. Westerterp, Chem. Eng. Sci. 54 (1999) 3291.
[7] L. Noristi, E. Marchetti, G. Baruzzi, P. Sgarzi, J. Polym. Sci. A: Polym. Chem. 32 (1994) 3047.
[8] X. Zheng, J. Loss, Macromol. Symp. 236 (2006) 249.
[9] X. Zheng, M.S. Pimplapure, G. Weickert, J. Loos, e-Polymers 28 (2006).
[10] M. Kakugo, H. Sadatoshi, M. Yokoyama, K. Kojima, Macromolecules 22 (1989) 547.
[11] M. Kakugo, H. Sadatoshi, J. Sakai, M. Yokoyama, Macromolecules 22 (1989) 3172.
[12] M. Abboud, P. Denifl, K.-H. Reichert, Macromol. Mater. Eng. 290 (2005) 1220.
[13] M. Abboud, P. Denifl, K.-H. Reichert, Macromol. Mater. Eng. 290 (2005) 558.
[14] M. Abboud, P. Denifl, K.-H. Reichert, J. Appl. Polym. Sci. 98 (2005) 2191.
[15] G. Fink, B. Tesche, F. Korber, S. Knoke, Macromol. Symp. 173 (2001) 77.
[16] W.C. Conner, S.W. Webb, P. Spenne, K.W. Jones, Macromolecules 23 (22) (1990) 4742.
[17] Z. Grof, J. Kosek, M. Marek, AIChE J. 51 (7) (2005) 2048.
[18] Z. Grof, J. Kosek, M. Marek, Ind. Eng. Chem. Res. 44 (2005) 2389.
[19] A. Di Martino, J.P. Broyer, R. Spitz, G. Weickert, T.F. McKenna, Macromol. Rapid Commun. 26 (2005) 215.
[20] M.A. Ferrero, M.G. Chiovetta, Polym. Eng. Sci. 31 (12) (1991) 904.
[21] M.A. Ferrero, M.G. Chiovetta, Polym. Eng. Sci. 27 (19) (1987) 1436.
[22] E.J. Nagel, V.A. Klrillov, W.H. Ray, Ind. Eng. Chem. Prod. Res. Dev. 19 (1980) 372.
[23] W.R. Schmeal, J.R. Street, AIChE J. 17 (5) (1971) 1188.
[24] M. Bartke, in: J.R. Severn, J.C. Chadwick (Eds.), Tailor-Made Polymers. Via Immobilization of Alpha-Olefin Polymerization Catalyst, Wiley–VCH Verlag GmbH & Co. KGaA, Weinheim, 2008.
[25] G. Cecchin, E. Marchetti, G. Baruzzi, Macromol. Chem. Phys. 202 (2001) 1987.
[26] B. Horáčková, Z. Grof, J. Kosek, Chem. Eng. Sci. 62 (2007) 5264.
[27] H. Hammawa, S.E. Wanke, J. Appl. Polym. Sci. 104 (2007) 514.
[28] T. Leinonen, P. Denifl, EP Patent 1,273,595 A1 (2003), to Borealis Technology Oy.
[29] P. Denifl, T. Leinonen, Patent WO 2004/029112, to Borealis Technology Oy.
[30] T. Garoff, T. Leinonen, Patent WO9219658 (1992), to Neste Oy.
[31] H.-L. Rönkkö, H. Knuuttila, P. Denifl, T. Leinonen, T. Venäläinen, J. Mol. Catal. A: Chem. 278 (2007) 127.
[32] A. Andoni, J.C. Chadwick, H.J.W. Niemantsverdriet, P.C. Thüne, J. Catal. 257 (2008) 81.
[33] A. Andoni, J.C. Chadwick, H.J.W. Niemantsverdriet, P.C. Thühe, Macromol. Rapid. Commun. 28 (2007) 1466.
[34] A. Andoni, J.C. Chadwick, H.J.W. Niemantsverdriet, P.C. Thüne, Macromol. Symp. 260 (2007) 140.